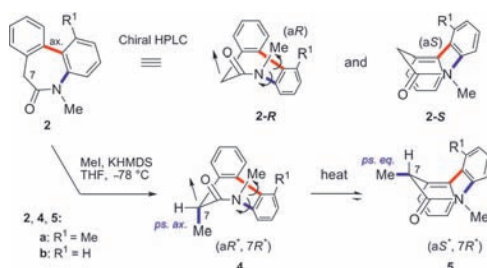


Atropisomeric Properties of the
Dibenzo[*b,d*]azepin-6-one NucleusHidetsugu Tabata,[†] Kumi Akiba,[†] Shoukou Lee,[‡] Hideyo Takahashi,[†] and
Hideaki Natsugari^{*†}*School of Pharmaceutical Sciences, Teikyo University, 1091-1 Sagamiko, Sagamihara,
Kanagawa 229-0195, Japan, and Graduate School of Pharmaceutical Sciences, The
University of Tokyo, 7-3-1 Hongo, Bunkyo-ku, Tokyo 113-0033, Japan*

natsu@pharm.teikyo-u.ac.jp

Received August 22, 2008

ABSTRACT



Dibenzo[*b,d*]azepin-6-ones (**2a,b**) were separated by chiral HPLC into the *aR*- and *aS*-atropisomers with high stereochemical stability, and methylation at C7 of **2a** stereoselectively gave the (*aR*^{*}, 7*R*^{*}) isomer (**4a**), which converted to the thermodynamically stable (*aS*^{*}, 7*R*^{*}) atropisomer (**5a**) after heating.

In the course of our research aimed at developing new γ -secretase inhibitors, we have been interested in LY-411575 (**1**)¹ and prepared several new derivatives (e.g., **1a**).² Our recent interest in relationships between axial chirality and biological activity³ also prompted us to elucidate the stereochemistry of the dibenzo[*b,d*]azepin-6-one moiety that constitutes the scaffold of LY-411575. The stereochemistry is of interest in that, in addition to the one asymmetric center

at C7, the moiety has chirality based on the sp^2 – sp^2 axis arising from a biphenyl (Figure 1). The literature related to LY-411575 reported that the 7*S* stereochemistry is important for potent activity.⁴ However, the stereochemistry on the dibenzo[*b,d*]azepin-6-one moiety has thus far not been

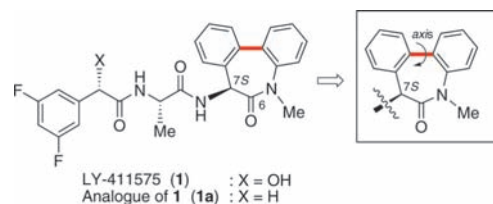


Figure 1. Structure of LY-411575 and its analogue.

clarified. Herein, we describe a study of the atropisomeric properties of the dibenzo[*b,d*]azepin-6-one nucleus.

In order to elucidate the effect of the axis on the stereochemistry, we prepared dibenzo[*b,d*]azepin-6-ones

[†] Teikyo University.

[‡] The University of Tokyo.

(1) (a) Lanz, T. A.; Hosley, J. D.; Adams, W. J.; Merchant, K. M. *J. Pharmacol. Exp. Ther.* **2004**, *309*, 49–55. (b) Lanz, T. A.; Fici, G. J.; Merchant, K. *J. Pharmacol. Exp. Ther.* **2005**, *312*, 399–406. (c) Best, J. D.; Jay, M. T.; Out, F.; Ma, J.; Nadin, A.; Ellis, S.; Lewis, H. D.; Pattison, C.; Reilly, M.; Harrison, T.; Shearman, M. S.; Williamson, T. L.; Attack, R. *J. Pharmacol. Exp. Ther.* **2005**, *313*, 902–908.

(2) (a) Fuwa, H.; Okamura, Y.; Morohashi, Y.; Tomita, T.; Iwatsubo, T.; Kan, T.; Fukuyama, T.; Natsugari, H. *Tetrahedron Lett.* **2004**, *45*, 2323–2326. (b) Morohashi, Y.; Kan, T.; Tominari, Y.; Fuwa, H.; Okamura, Y.; Watanabe, N.; Sato, C.; Natsugari, H.; Fukuyama, T.; Iwatsubo, T.; Tomita, T. *J. Biol. Chem.* **2006**, *281*, 14670–14676. (c) Fuwa, H.; Takahashi, Y.; Konno, Y.; Watanabe, N.; Miyashita, H.; Sasaki, M.; Natsugari, H.; Kan, T.; Fukuyama, T.; Tomita, T.; Iwatsubo, T. *ACS Chem. Biol.* **2007**, *2*, 408–411.

(**2a–d**) (Figure 2). Starting from the coupling reaction of 2-bromo-3-methylaniline (or 2-bromoaniline) and 2-iodophenylacetonitrile, the dibenzoazepinones **2a**, **2c**, and **2d** were

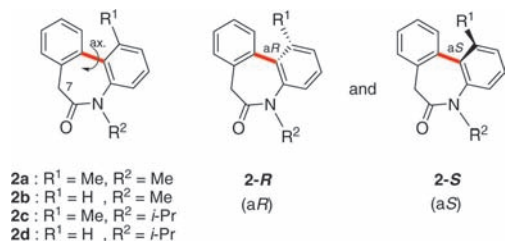


Figure 2. Conformation of the dibenzo[*b,d*]azepin-6-one structure.⁵

easily prepared in three steps (i.e., hydrolysis–lactam formation, and *N*-alkylation) according to the procedure used for the synthesis of **2b** ($R^1 = \text{H}$).^{2a,6} Compounds **2a** and **2c** have a methyl group at the ortho position on the benzene ring ($R^1 = \text{Me}$), which provides a high rotation barrier for the axis. Similarly, compounds **2c** and **2d** have a bulky *N*-isopropyl group ($R^2 = i\text{-Pr}$), which is aligned to make the molecule more rigid by introducing steric hindrance around the amide moiety.

As mentioned above, the dibenzo[*b,d*]azepin-6-ones (**2a–d**) should have chirality based on the sp^2 – sp^2 axis arising from the biphenyl and thus are anticipated to occur in the racemic form of the enantiomers, i.e., (**2-R**: *aR*) and (**2-S**: *aS*). Compounds **2a–d** were separated into the respective enantiomers with HPLC using a chiral column (CHIRAL-PAK AD-H), and these enantiomers were successfully isolated using preparative HPLC. Fortunately, single crystals for the X-ray crystal structure analysis of both enantiomers of **2a** ($R^1 = R^2 = \text{Me}$) were obtained. Thus, the configuration of **2a-R** [$[\alpha]_D -92.0$ (*c* 0.3, MeOH)] was ascertained to be *aR* and that of **2a-S** [$[\alpha]_D +93.7$ (*c* 0.3, MeOH)] to be *aS* as shown in Figure 3.

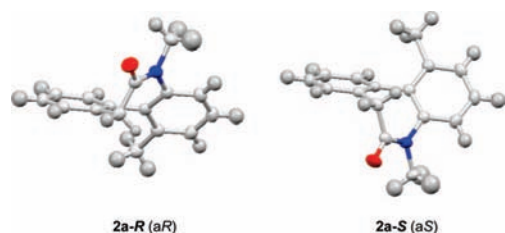


Figure 3. X-ray crystal structures of enantiomers **2a-R** and **2a-S**.

The X-ray analysis also revealed that, in addition to the chirality based on the axis of the biphenyl moiety, **2a** has another axial chirality arising from the sp^2 – sp^2 axis of the benzene–amide bond. Although latent in the molecule, the latter axial chirality actually exists. The configuration of the enantiomers **2a-R** and **2a-S** was shown to be (*aR,aS*) and

(*aS,aR*), respectively (see the structures in Table 1). Taking into consideration the fact that no diastereomers of **2a–d** are observed using NMR and HPLC, the latter axis is

Table 1. Stability of the Separated Dibenzo[*b,d*]azepin-6-one Enantiomers **2-R** and **2-S**⁵

2-R/2-S	R^1	R^2	ΔG^\ddagger (kcal/mol) (kJ/mol)	racemization in toluene
a	Me	Me	29.3 (122)	110 °C, 2 h
b	H	Me	23.4 (98)	37 °C, 2 h
c	Me	<i>i</i> -Pr	32.7 (137)	150 °C, 4 h ^a
d	H	<i>i</i> -Pr	25.3 (106)	50 °C, 6 h

^a Solvent is DMF.

presumed to move together like a gear with the axis at the biphenyl to form the stable relative configuration of (*aR*,aS**) in the dibenzoazepinone nucleus. The presumption is also supported by the molecular modeling of **2a**, in which the relative configuration of (*aR*,aS**) is readily built up, while that of (*aR*,aR**) is not built up because of the large strain.

Next, the stereochemical stability of these separated enantiomers of **2a–d** was examined. Table 1 shows the activation free-energy barrier to rotation (ΔG^\ddagger)⁷ and the conditions required for racemization of the enantiomers. The enantiomers of **2a** (**2a-R** and **2a-S**) ($R^1 = R^2 = \text{Me}$) showed high stereochemical stability with a ΔG^\ddagger value of 29.3 kcal/mol. On the other hand, the enantiomers of **2b** (**2b-R** and **2b-S**) ($R^1 = \text{H}$, $R^2 = \text{Me}$), which are less restricted at the axis of the biphenyl, were less stable ($\Delta G^\ddagger = 23.4$ kcal/mol). Higher stereochemical stability was observed for the

(3) (a) Ikeura, Y.; Ishimaru, T.; Doi, T.; Fujishima, A.; Natsugari, H. *Chem. Commun.* **1998**, 2141–2142. (b) Natsugari, H.; Ikeura, Y.; Kamo, I.; Ishimaru, T.; Ishichi, Y.; Fujishima, A.; Tanaka, T.; Kasahara, F.; Kawada, M.; Doi, T. *J. Med. Chem.* **1999**, *42*, 3982–3993. (c) Ishichi, Y.; Ikeura, Y.; Natsugari, H. *Tetrahedron* **2004**, *60*, 4481–4490. (d) Tokitoh, T.; Kobayashi, T.; Nakada, E.; Inoue, T.; Yokoshima, S.; Takahashi, H.; Natsugari, H. *Heterocycles* **2006**, *70*, 93–99.

(4) Wong, G. T.; Manfra, D.; Poulet, F. M.; Zhang, Q.; Josien, H.; Bora, T.; Engstrom, T.; Pinzon-Ortiz, M.; Fine, J. S.; Lee, H. J.; Zhang, L.; Higgins, G. A.; Parker, E. M. *J. Biol. Chem.* **2004**, *279*, 12876–12882.

(5) For convenience, solid bold and broken arrowheads are used for the enantiomerically pure forms to show the absolute stereochemistry and bold solid and broken lines are used for racemic compounds to show the relative stereochemistry.

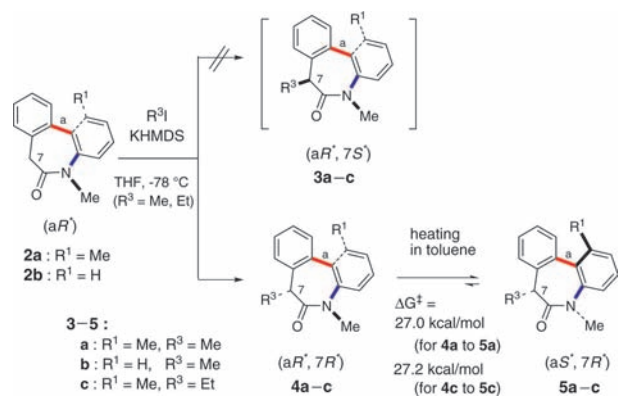
(6) Baudoin, O.; Cesario, M.; Guenard, D.; Gueritte, F. *J. Org. Chem.* **2002**, *67*, 1199–1207.

(7) The ΔG^\ddagger value was determined on the basis of the time-dependent conversion rate (% ee) estimated from chiral HPLC analysis of a solution of the enantiomers after being allowed to stand at designated temperatures (see the Supporting Information for measurements); see: Petit, M.; Lapiere, A. J. B.; Curran, D. P. *J. Am. Chem. Soc.* **2005**, *127*, 14994–14995.

N-isopropyl derivatives (**2c,d**) compared with the *N*-methyl derivatives (**2a,b**). That is, the enantiomers of **2c** ($R^1 = \text{Me}$, $R^2 = i\text{-Pr}$), which are in the most sterically restricted form, were extremely stable ($\Delta G^\ddagger = 32.7$ kcal/mol). The enantiomers of **2d** ($R^1 = \text{H}$, $R^2 = i\text{-Pr}$) were also more stable than those of the corresponding **2b**. The increased energy barrier (**2c** vs **2a** and **2d** vs **2b**) is obviously ascribed to the *N*-isopropyl group. These data also indicate that latent chirality about the axis based on the benzene–amide bond occurs, and the two axes (at the biphenyl and benzene–amide) move together like a gear during the isomerization.

We further examined the substituent effect at the seven-membered ring on the stereochemistry of the dibenzoazepinones (**2a,b**). Thus, compound **2a** was methylated (MeI/KHMDS in THF at -78 °C) to introduce an asymmetric center at the C7-position (Scheme 1). Two diastereoisomers,

Scheme 1. Highly Stereoselective Alkylation at the C7-Position of **2** and Isomerization of **4** to **5**⁸



3a and **4a**, were expected to be produced by this methylation. Contrary to expectations, however, only one diastereomer (**4a**) was obtained in 98% yield. This result indicates that the conformation defined by the axial chiralities controlled the stereochemistry of the methylation at C7 of **2a**. Compound **4a** was stable in a solution at room temperature, but at elevated temperatures gradually converted to the atropisomeric diastereomer (**5a**)⁸ (= the enantiomeric form of **3a**). The conversion was temperature dependent, i.e., the ratio of **4a**:**5a** after **4a** had been allowed to stand for 2 h in toluene at 37 °C was ca. 96:4 and at 80 °C was ca. 42:58. The conversion reached equilibrium in a ratio of ca. 3:97 after ca. 0.5 h of storage in toluene at 110 °C.⁹ The interconversion barrier (ΔG^\ddagger) between **4a** and **5a** was calculated to be 27.0 kcal/mol. Similarly, the alkylation of **2a** with EtI in place of MeI gave the C7-ethyl derivative **4c**, which underwent isomerization to **5c** after heating in toluene ($\Delta G^\ddagger = 27.2$ kcal/mol). The conversion reached equilibrium in a ratio of ca. 1:99 (**4c**:**5c**) after **4c** had been allowed to stand in toluene

(8) Heating a toluene solution of **4a** at 110 °C in the presence of a small amount of D_2O for 2 h did not give the H–D exchange product but only gave **5a**, which indicates that the configuration at C7 of **4a** was preserved and the isomerization occurred at the axes.

at 110 °C. The slight difference in the ratios in the equilibrium state between **4a–5a** and **4c–5c** may be due to the difference in the bulkiness of the substituent (Me vs Et); i.e., the larger substituent at C7 in **4** may allow lowering the stability of **4** to increase **5** in the equilibrium state. On the other hand, the only product isolated by the methylation of **2b** ($R^1 = \text{H}$, $R^2 = \text{Me}$) was the thermodynamically stable isomer **5b**. However, detailed investigation of the reaction using TLC and ^1H NMR showed that the unstable isomer (**4b**) was initially formed,¹⁰ which readily isomerized to give **5b** during workup even at low temperature (ca. 10 °C) (Scheme 1).

The structures of **4a** and **5a** were determined using NOE analysis (Figure 4). In **4a**, NOEs were observed between two

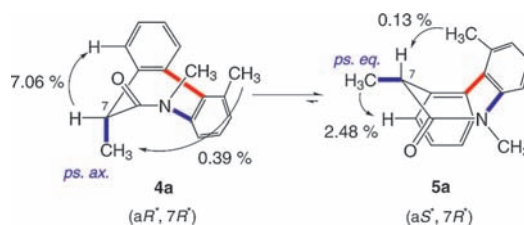


Figure 4. NOE analysis of **4a** and **5a**.

methyl groups and between two protons, where the C7-methyl is in the pseudoaxial orientation. On the other hand, in **5a**, the NOEs observed were between the C7-methyl and benzene-H and between the C7-H and benzene-methyl, where the C7-methyl is in the pseudoequatorial orientation. Thus, the stereochemistry of **4a** was determined to be (aR^* , $7R^*$) and that of **5a** (aS^* , $7R^*$).

The highly stereoselective methylation of **2a** to **4a** is explained by the kinetically controlled reaction. A plausible mechanism of the methylation of **2a** is illustrated in Figure 5. As shown in Figure 5, steric hindrance of the benzene

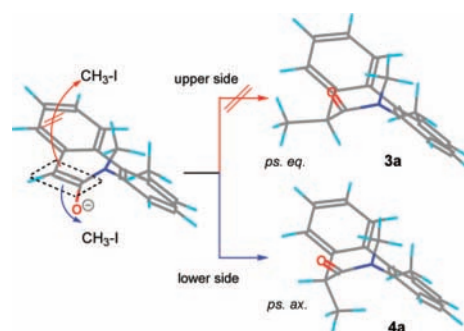


Figure 5. Mechanism of highly stereoselective methylation.

ring and the *N*-methyl group covers the upper side of the enolate so that the electrophile should come only from the lower side to form **4a**. Therefore, the conformation based on the axial chiralities completely controlled the stereochem-

istry at C7 in methylation. It should be noted that the product **4a** possesses the methyl group in the pseudoaxial orientation, which is thermodynamically unstable. On the other hand, the thermal atropisomerization from **4a** to **5a** is well explained by the fact that **5a** with a pseudoequatorial methyl group is thermodynamically more stable than **4a** with a pseudoaxial methyl group. It is noteworthy that the introduction of the alkyl group at C7 clearly lowered the ΔG^\ddagger value [i.e., 29.3 kcal/mol (from **2a-R** to **2a-S**) (Table 1) vs 27.0 kcal/mol (from **4a** to **5a**) and 27.2 kcal/mol (from **4c** to **5c**) (Scheme 1)]. This result indicates that atropisomerism is markedly affected by the stereochemical stability of the entire molecule, i.e., the conformational change at the C7-alkyl group from pseudoaxial to pseudoequatorial affects the rate of atropisomerism to lower the rotational barrier.

In conclusion, the stereochemical and physicochemical properties of the dibenzo[*b,d*]azepin-6-one derivatives (e.g., **2**, **4**, and **5**) were clarified. The two sp^2-sp^2 axes in the dibenzazepinone nucleus move together like a gear to form one diastereomer with a stable relative configuration. Owing to the axial chiralities in **2**, the kinetically controlled alkylation first proceeded, and then atropisomerization occurred to form thermodynamically more stable molecules. Based on these results, studies on the C7-amino derivatives of **2**, which are more closely related to LY-411575, are

currently in progress. We believe that this study will contribute to the creation of new drug candidates with this type of scaffolds, which may lead to the development of drugs for Alzheimer's disease and other conditions. Although often overlooked, the axial chiralities are latent in many molecules. They may exert a strong influence not only on the stereochemical features of the molecules but also on biological activity.

Acknowledgment. We thank Sagami Chemical Research Center for X-ray analysis. This work was supported in part by a Grant-in-Aid for Scientific Research (19590108) from the Japan Society for the Promotion of Sciences. Continuous support by Takeda Pharmaceutical Co. Ltd. is gratefully acknowledged.

Supporting Information Available: Experimental procedures, spectral data for all compounds, and X-ray crystal data (CIF) for **2a-R** and **2a-S**. This material is available free of charge via the Internet <http://pubs.acs.org>.

OL801968B

(9) The ratio was determined by HPLC using a nonchiral column (YMC-Pack SIL-06).

(10) See the Supporting Information for the ^1H NMR spectrum of the crude mixture of **5b**, which was measured immediately after workup of the reaction.